

Thermo-Mechanical Modelling and Experimental Verification of Distortion and Residual Stress for S355J2G3 Plate Welded by using Different Filler

Muhammad Faisal Nadeem, Bilal Ahmed

Abstract—Welding residual stresses are considered one of the most insidious forms of stresses which can affect integrity of structures. Residual stresses are difficult to measure physically and estimate theoretically. High tensile stresses can often lead to loss of performance in corrosion, fatigue and fracture. This paper presents development of a Finite Element Model using commercially available tool SYSWELD, to analyze the effect of changing filler configuration on the nature of welding residual stresses and distortion in S355J2G3 material. An S355J2G3 plate of 250x100x3mm dimensions is butt welded without filler and with ER70S6 filler.

The results have been experimentally verified to validate the developed Finite Element Model. Blind hole drilling method is used for the measurement of residual stresses experimentally. The results indicate quite high tensile residual stresses developed in the molten zone for welding the plate without filler as compared to the case for welding with ER70S6 filler. A lesser distortion results when S355J2G3 plate is welded autogenously. The experimental & finite element analysis results show good agreement for the predicted residual stresses and distortion.

Keywords—Finite element method, Weld distortion, Residual stresses, Hole drill method, Temperature distribution, filler

I. INTRODUCTION

WELDING is the most efficient way to join metals. It is considered a complex manufacturing process where number of variables are not easily understood and appreciated. Welding find its application in the products made of metals. Industries including building construction, aerospace structures, automobiles, ship building, storage tank construction, nuclear reactors, etc. [1].

However in spite of its many advantages, welding is almost always accompanied by residual stresses and distortion[2]. Welding Residual stresses occur due to non-uniform temperature distribution caused by localized heating. Residual stresses in weldments can be detrimental to integrity and service behavior as they cause premature failure or distortion or both.

Manuscript received April 09, 2019.

M. Faisal Nadeem is with the Pakistan Space & Upper Atmosphere Research Commission, Pakistan (+92-342-2523558; e-mail: mfaisaln@gmail.com).

Bilal Ahmed is with the Pakistan Space & Upper Atmosphere Research Commission, Pakistan (e-mail: bilal.ahmeds@yahoo.com)

Welding distortion often results in problems such as dimensional inaccuracies during assembly and therefore may increase cost of the product [2].

Prediction of residual stresses caused by welding and estimation of resulting distortion can therefore offer significant advantages in terms of cost and quality of welded products.

Finite element analysis proved to be an efficient and powerful way to evaluate through-thickness residual stresses measurement in girth welded pipes and to simulate the strain gauge data obtained through experiments [3]. Y. Shim developed an analytical method for predicting through thickness distribution of residual stresses in a thick plate with a multi-pass welding process [4].

Welding in high strength steel produces very high stress gradient in fusion zone, which result in cold cracks. This problem can be minimized in the high strength steel by controlling the weld heat input [5]. For high strength carbon steel butt welds, in order to obtain results using the finite element method very close to the results obtained in experiments, different mesh sizes could be taken into consideration [6]. Weld heat input in high strength steel causes stress gradient, resulting in cold crack occurring at the fusion zone. Stress calculation is necessary because high residual stresses may be caused fractures, fatigue which causes unpredictable failures in regions near the weld bead region [7].

The distribution of the residual stress in the weld zone of austenitic stainless steel in the direction of the width of test plate has highest influence on the formation of cold cracks [8]. Phase transformation study revealed that for low carbon steel-martensite formation and high transformation temperature- has an insignificant effect on the welding residual stress and the distortion while for medium carbon steel, it has significant effect [9]. Residual stresses and distortion values increase with of laser beam power. On the other hand, the distortion and residual stresses decrease as the speed increases. There is a reduction of residual stress and distortion values as the spot diameter increases [10].

Due to the shrinkage and deformation in the weld zone of the TIG welded stainless steel pipes, a high compressive stress is developed on the outer surface and a tensile residual stress is developed on the inner surface and at a particular point it diminishes completely. The range of residual stress distribution became wider when welding current increases [11].

The maximum tensile and compressive stresses are created in the inner surface of the pipe; therefore, this surface is susceptible of cracks resulted from welding residual stress [12].

Heat effected zone play pivotal role in determining the strength of a welded joint which changes the properties of parent material and reduce the strength after welding operation. There are many case for which fatigue life of the welded joints are a major design consideration for those structures under continuously cyclic loading [13]. Side heating (SH) can successfully reduce out-of-plane deformation. The areas beneath the burners in DP600 show a lower micro-hardness than the base metal, mainly because of tempering the martensite. The welding with SH does not reduce the compressive stresses ahead of the weld zone, nor does it increase the tensile stress in the weld zone during cooling. The tensile stresses generated by the burners redistribute the final residual stresses [14].

Dissimilar material's welding, such as, carbon steel and stainless steel, is widely used in power plant. A lot of stress corrosion cracking (SCC) occurred in the weld joint, which are affected greatly by residual stresses. With the increase of heat input, the residual stress and plastic deformation around the weld root increases. Low heat input is recommended for the welding between 0Cr18Ni9 steel (ASTM 304) and 20 carbon steel (AISI 1020) [15]. The higher tensile residual stress occurred within or in the proximity of the buttering and the Dissimilar Metal Welding (DMW) region toward the outer surfaces, while compressive stress distribution showed the opposite. In addition, stress magnitudes were found higher in DMW than in Similar Metal Welding (SMW) [16].

Many researchers [3-16] have done a lot of work for evaluation & analysis of residual stresses and distortion using FEA and experimental techniques for different materials. However, effect of changing filler configuration on generation of residual stresses and distortion in the welding of low alloy steel such as, S355J2G3 has not been analyzed.

This work deals with the study of development of residual stresses in weld zone by changing the filler while keeping the same base metal. For this finite element modeling and experimental validation of distortion and residual stresses has been carried out for: when S355J2G3 is butt welded a) with S355 filler; b) with ER70S6 filler.

II. EXPERIMENTAL WORK

Experiments have been performed on two S355J2G3 plates having dimensions 200 mm x 250 mm x 3mm thick using TIG welding process. The test pieces are designated as Test piece #1 (TP1) for S355J2G3 welded autogenously (S355) and Test piece # 2 (TP2) for S355J2G3 welded using ER70S6 filler. The chemical composition for Base Metal and Filler Wire used in this study is tabulated in Table I. Table II contains the optimized parameters for the TIG welding. 99.9% pure Argon Gas is used for shielding purpose.

Table I
Chemical composition of base metal and filler wire

| | Base Metal | Filler Wire |
|-----------|------------|-------------|
| | S355 | ER70S6 |
| <i>C</i> | 0.12 | 0.09 |
| <i>Mn</i> | 0.63 | <1.60 |
| <i>Si</i> | 0.13 | 0.9 |
| <i>S</i> | 0.01 | 0.007 |
| <i>P</i> | 0.02 | 0.007 |
| <i>Ni</i> | 0.02 | 0.05 |
| <i>Cr</i> | 0.01 | 0.05 |
| <i>Mo</i> | 0.01 | 0.05 |
| <i>Cu</i> | 0.01 | 0.2 |
| <i>V</i> | <0.01 | 0.05 |

Table II
CHEMICAL COMPOSITION OF BASE METAL AND FILLER WIRE

| WELDING PARAMETER | TEST PIECE # 1 (TP1) | TEST PIECE # 2 (TP2) |
|------------------------------|-------------------------|-------------------------|
| | BASE METAL: S355J2G3 | BASE METAL: S355J2G3 |
| | FILLER: S355J2G3 | FILLER: ER70S6 |
| <i>Current (Ampere)</i> | 190 (150~ 190) | 150(147~150) |
| <i>Voltage (Volt)</i> | 12.6 | 12.7 |
| <i>Speed (mm/sec)</i> | 3.2 | 3.2 |
| <i>WFS (mm/sec)</i> | -Not Applicable- | 6.38 |
| <i>Heat Input (J/mm)</i> | 590 | 595 |

Welding is carried out using a Multi-Process Power Supply (Miller - Phoenix 456CC/CV DC Inverter Arc Welder). Specially designed welding jig (Fig. 1) has provided the clamping and restraint to test pieces during the welding process. A copper plate has been placed beneath the welded pieces of plate. It has hole through which argon was flowing at the rate of 20 ~ 25 cfh.



Fig. 1. Experimental Setup for Welding (Specially designed welding jig for clamping)

A. Thermal History (Temperature Profile) Record

Fig. 2 shows the location of 03 x thermo-couple employed transverse to Weld Centre Line (WCL) for recording temperature history during the experimental work.

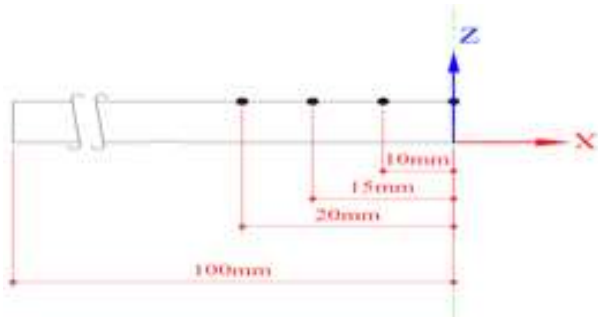


Fig.2. Location of Thermo-Couple for Thermal History Measurements

Thermal History has been recorded using Data Acquisition Card Addi-Data 3200APX with Addi-Reg Software. Fig. 3 & 4 depicts temperature variation along the selected nodes. One can observe that as the transverse distance from the seam increases, the node peak temperature and rate of temperature change gradually decreased.

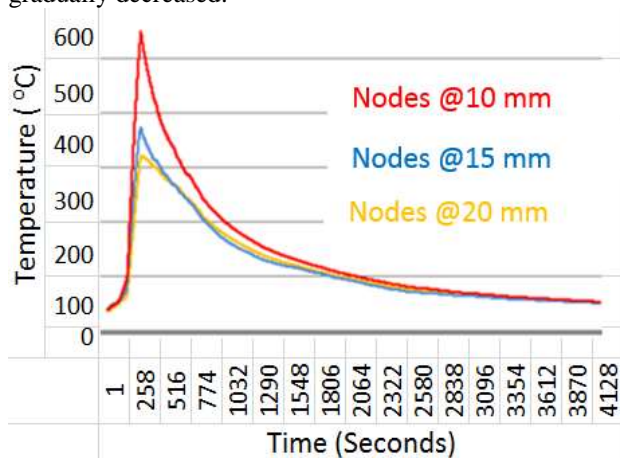


Fig.3. Thermal History for TP1 –S355J2G3 Autogenously Welded (S355 Filler)

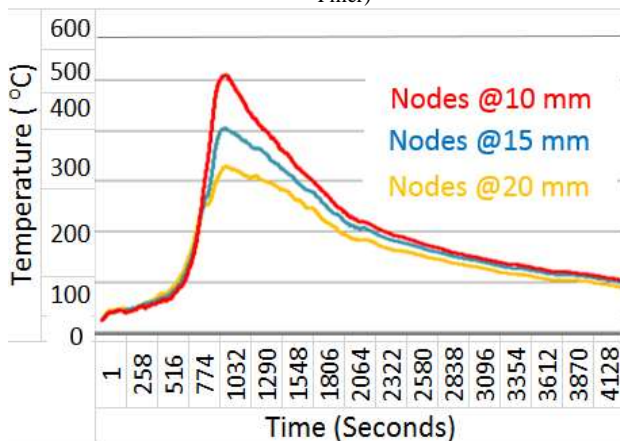


Fig. 4. Thermal History for TP2 –S355J2G3 welded with ER70S6 Filler

A. Residual Stress Measurement using Hole Drilling Method

The hole-drilling method is a convenient and effective method for measuring residual stresses. The basic principle was first proposed by Mathar in 1934 [17]. Since that time, many researchers [17-21] have further developed the method, culminating in the establishment of a standardized procedure ASTM E837.

The original and most common objective of hole-drilling measurements is to evaluate in-plane residual stresses that can be assumed to be uniform either with depth from the surface of a thick specimen, or through the thickness of a thin specimen. ASTM Standard Procedure E837 refers to these cases. Over the years, several mathematical methods have been developed for calculating non-uniform residual stresses in thick materials from hole-drilling measurements [19].

These methods seek to identify the interior residual stresses by considering the evolution of the strains measured as the depth of the drilled hole is gradually increased. Because the strain measurements are made from strain gages attached to the specimen surface, the greatest sensitivity is to the residual stresses close to the surface. Sensitivity rapidly reduces with depth. At depths beyond about half the mean diameter of the hole-drilling rosette, sensitivity to the interior stresses completely disappears.

The three stress calculation methods (Uniform Stress, Power Series and Integral Method) used by H-DRILL span the range between low sensitivity to experimental errors and high spatial resolution of calculated residual stresses. A “Blind-Hole” type of measurement is used when working with materials that are thick as compared with the rosette size. The material thickness should exceed 1.2 times the mean diameter of the hole-drilling rosette that is used. Table III describes the parameters for Rosette Type and Blind hole dimensions used during this work.

| ROSETTE TYPE | MIN. THICKNESS | MIN. HOLE DIAMETER | MAX. HOLE DIAMETER |
|--------------|----------------|--------------------|--------------------|
| 062RE | 6.16mm | 1.52mm | 2.54mm |

In this work, residual stress measurement is carried out using Hole Drill Method as per ASTM E837. The equipment utilized is the Vishay Instrument’s H-Drill Residual Stress Milling Guide Model RS-200, along with H-Drill Residual Stress Calculation Program Version 2.22[19].

Typical arrangement for strain gauges and hole drilling by milling guide is shown in Fig. 5 and Fig. 6, respectively.

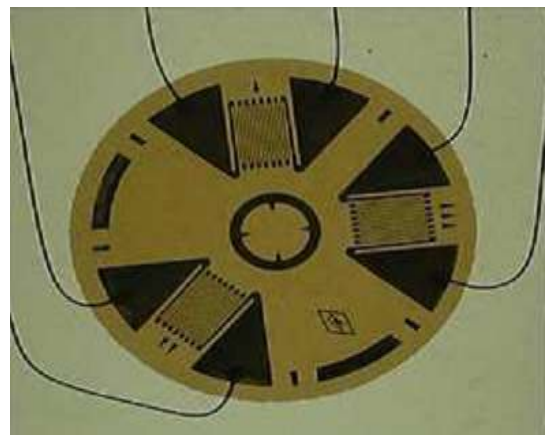


Fig.5. Typical Strain Gauge Arrangement for Residual Stress Measurements



Fig.6. Typical Residual Strain Measurements Setup by the Blind Hole Drilling Method

The results of the residual stresses obtained using hole-drill methods for two different cases are tabulated in Table No. IV and Table No. V.

Table IV
MEASURED RESIDUAL STRESS VALUES - TP1 – 8MM FROM WELD CENTERLINE

| DEPTH mm | S _{MAX} MPa | S _{MIN} MPa | T _{MAX} MPa | β Deg | S1 MPa | S3 MPa | T13 MPa |
|----------------------|-------------------------|-------------------------|-------------------------|----------|-----------|-----------|------------|
| Overall up to 1.2 mm | 481 | 89 | 196 | -85 | 91 | 478 | 31 |
| 0.25 | 298 | 45 | 127 | -85 | 47 | 297 | 21 |
| 0.5 | 544 | 84 | 230 | 89 | 84 | 544 | -6 |
| 0.75 | 471 | 84 | 193 | -86 | 86 | 469 | 29 |

S_{max} and S_{min} are the two principal stresses, and β is the angle measured clockwise from the direction of gage 1 to the direction of the maximum (most tensile) principal stress S_{max}. T_{max} is the maximum shear stress that is present. It acts in the directions midway between the two principal directions. S1 is the axial stress in the direction of gage 1, S3 is the axial stress in the direction of gage 3, and T13 is the in-plane shear stress in directions of gages 1 and 3.

Table V
MEASURED RESIDUAL STRESS VALUES – TP2 – 10MM FROM WELD CENTERLINE

| DEPTH mm | S _{MAX} MPa | S _{MIN} MPa | T _{MAX} MPa | β Deg | S1 MPa | S3 MPa | T13 MPa |
|----------------------|-------------------------|-------------------------|-------------------------|----------|-----------|-----------|------------|
| Overall up to 1.2 mm | 462 | 168 | 147 | -53 | 273 | 357 | 141 |
| 0.25 | 155 | 61 | 47 | -54 | 93 | 123 | 45 |
| 0.5 | 124 | 20 | 52 | -78 | 24 | 120 | 21 |
| 0.75 | 259 | 105 | 77 | -50 | 168 | 196 | 76 |

B. Distortion Measurement

A Coordinate Measurement Machine (CMM) has been utilized for accurate measurement of distortion caused by welding for each case of TP1 & TP2 respectively. A grid of 25 x 25 mm has been drawn on each specimen surface and measurements are carried out using the CMM on each grid-point.

C. Distortion Plot for Each Case

Matlab® is used for plotting three dimensional surface plots using the values obtained from CMM for the distortion measurements. The resulting plot thus obtained for S355J2G3 welded autogenously is shown in the Fig. 7. The overall distortion for this case at the edges of the specimens comes out to be about 1~1.5 mm. The maximum distortion noted at the one corner is approx. about 3mm.

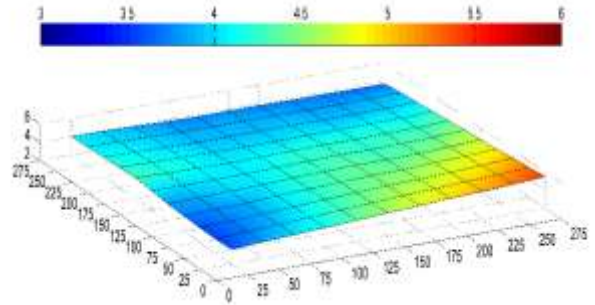


Fig.7. Distortion plot for S355J2G3 plate welded autogenously

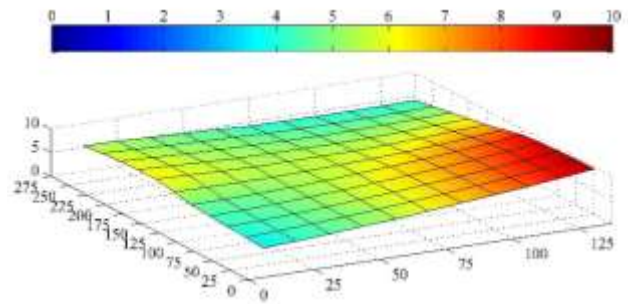


Fig.8. Distortion plot for S355J2G3 plate welded with ER70S6 Filler

Fig. 8 shows the surface plot for distortion measured using CMM when S355J2G3 is welded with ER70S6. The overall distortion recorded for this case is about 2.5 ~ 3mm. The maximum distortion at the one corner is approx. about 5~6mm.

III. FINITE ELEMENT ANALYSIS

In this paper, commercially available Finite Element Tool SYSWELD®2010.0 (as Solver & Post Processor) is being used to study & analyze the effect of change of filler configuration

Finite element meshed model has been developed utilizing Visual Mesh® (as a Pre-Processor). To save the computation time & resources involved, a symmetric model of having dimensions 100mmx250mmx3mm has been developed.

First of all, 2D mesh having cross-section (100 mm x 3 mm) been developed. Later on, these elements have been extruded to 250mm for generation of 3D finite elements (Fig. 13). Elements are of type 3020. All these new elements created are discretized into uniform 20-node hexahedron for the solution domain. These elements (type 3020) are shown in Fig. 9 with quadratic shape function perform extremely well for bending dominated cases and in general mechanics.

SYSWELD® needs specific groups to perform the thermo-mechanical analysis. In order to apply convection on the surfaces of the plate with its surroundings, two dimensional elements are extracted from the solid mesh. Then, for modeling

of heat source movement, the one-dimensional elements are extracted from 2D elements for trajectory as well as for reference purpose. There are totally 100 one dimensional elements generated from the two-dimensional mesh. For the fusion of weld metal with filler metal deposition, bead group having 3D elements is created.

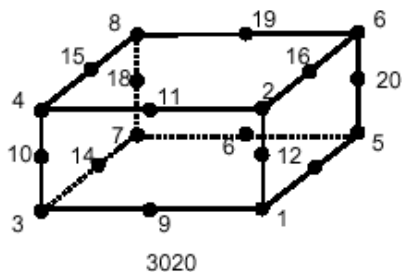


Fig.9. Element type used in Thermo-Mechanical Analysis

During meshing, special attention is given for finer mesh to be generated in the area of weld line and heat affected zone for taking into account of having large spatial temperature gradients, and rapid temperature fluctuations. A very small-time step is needed for analysis. For our case, we have chosen the mesh size 0.5 x 0.5 mm in the Molten Zone (MZ) & 1mm x 1mm in the Heat Affected Zone (HAZ). The rest of the plate has coarse mesh size varying from 1mm to maximum of 5mm at the extreme edge side.

To simulate the weld deposit, activation and de-activation of the proper elements has been implied with the use of simplified FORTRAN® subroutine available within the SYSWELD®. During Thermal Analysis, welding torch determine the sequence, when deactivated elements to be get reactivated. For the succeeding structural analysis, solidification temperature results in the birth of an element. For thermal expansion coefficients, filler and base metals melting and ambient temperatures are set as reference temperatures. S355J2G3 Thermo Mechanical Physical Properties used during FEA are plotted in Fig. 10.

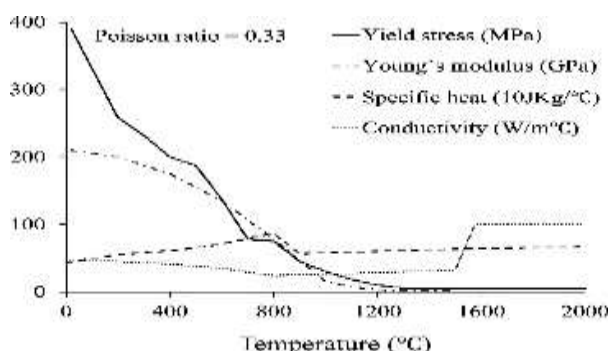


Fig.10. S355J2G3 Thermo Mechanical Physical Properties

The amount of heat transfer to the welded specimens for the TIG welding can be approximated by employing double ellipsoidal heat source (shown in Fig. 11) according to Nguyen et al.[22]. A double ellipsoidal heat source consists of Front and Rear ellipsoids. The heat density at an arbitrary point (x, y, z) within each one-half ellipsoid is described by the following equations (1) & (2):

$$Q_f(x, y, z) = \frac{6\sqrt{3}r_f Q}{a_h b_h c_{hf} \pi \sqrt{\pi}} e^{-3\left(\frac{x^2}{c_{hf}^2} + \frac{y^2}{a_h^2} + \frac{z^2}{b_h^2}\right)} \quad (1)$$

$$Q_b(x, y, z) = \frac{6\sqrt{3}r_b Q}{a_h b_h c_{hb} \pi \sqrt{\pi}} e^{-3\left(\frac{x^2}{c_{hb}^2} + \frac{y^2}{a_h^2} + \frac{z^2}{b_h^2}\right)} \quad (2)$$

Where, $a_h, b_h; c_{hf}; c_{hb}$ are the heat source parameters for the Front and Rear Ellipsoidal Heat Source.

Q = arc heat input = ηVI , η being the efficiency and V and I being the arc voltage and current respectively, and r_f, r_b are the proportional coefficients at the front and the back of the heat source, respectively, such that ($r_f + r_b = 2$.)

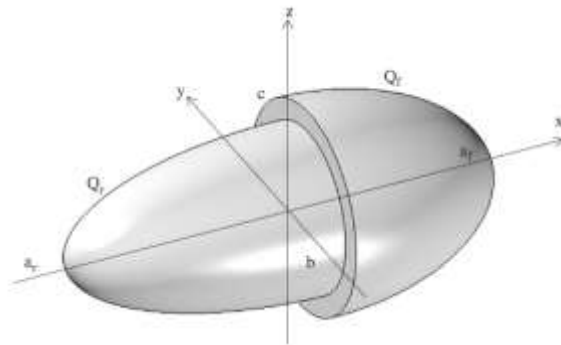


Fig.11. Double ellipsoidal heat source parameters designations as employed in SYSWELD® for Thermal Finite Element Analysis [22]

Following two sections describes the approach being employed in this paper. The important parameters have been analyzed using FEA tools and the same have been experimentally verified.

A. Thermal Analysis

This section consists of FEA simulation of welding thermal histories and associated temperature fields developed within the TP1 & TP2 during the welding process.

Several input parameters are necessary to consider for thermal analyses for defining the *boundary conditions*. Heating and cooling phase *depends significantly* upon *initial temperature of the specimen* as well as *ambient temperature*. The heat transfer phenomenon during TIG welding process is divided into two parts: *convection and radiation*. The heat exchange surfaces are defined by creating *surface element*. In this study, the *convective heat transfer coefficient of 25W/(m²K)* is applied. The emissivity coefficient (ϵ) is assumed to be 0.8 along with the definition of ambient temperature (T_{amb}) for *radiation*. The radiative heat transfer coefficient is described by cumulative heat transfer coefficients covering convection as well as radiation parameters.

B. Calibration of the heat source

The SYSWELD® suggested a well-established approach which is based on calibration of heat source using Heat Input Fitting Tool. This tool is used to model a FEA specimen with the same geometric details as the actual. After that, meshing and material properties are defined, along with the associated double ellipsoidal heat source parameters to simulate the heat transfer in the TIG welding process. Then quasi steady state

FEA simulation is run for an intermediate time step to obtain the FEA weld macro-graph by changing the double ellipsoidal heat source parameters.

Table VI
HEAT SOURCE CALIBRATION DATA

| HEAT SOURCE PARAMETERS | S355J2G3 (AUTOGENOUSLY) | S355J2G3 (WITH ER70S6) |
|------------------------|-------------------------|------------------------|
| Q_f | 18 | 17.83 |
| Q_r | 12 | 11.54 |
| A_f | 2 | 2 |
| b_h | 4 | 4 |
| C_{hf} | 5 | 5.5 |
| C_{hb} | 1.5 | 1.5 |
| x_o | 0 | 0 |
| y_o | 0 | 0 |
| z_o | 0 | 0 |
| a_y | 0 | 0 |
| Power | 910 | 935 |

This process is repeated until the metallurgical phases/zones like HAZ, Fusion zone & Weld Base Metal completely matches with the experimental macro-graph of actual welded specimens. The final double ellipsoidal heat source parameters for Finite Element analysis obtained are presented in Table VI. The Heat Source parameters thus obtained are used for performing Thermal & Mechanical Analysis of S355J2G3 plate for both cases respectively.

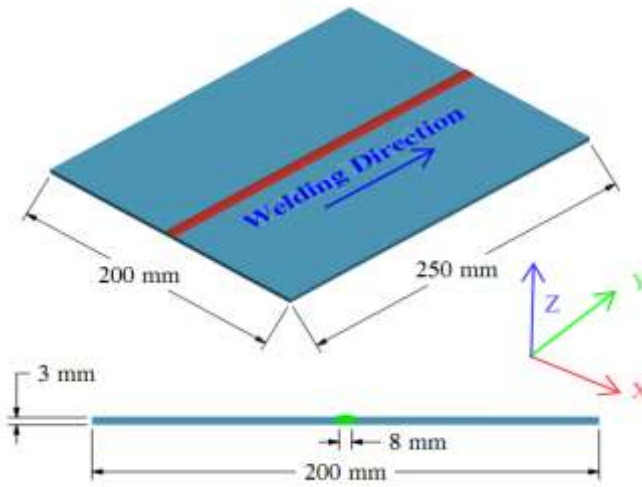


Fig.12. Elements types used in Analysis

For the transient simulation to complete, first thermal analysis is carried out followed by mechanical analysis. On the basis of the parameters defined in heat input fitting, transient analysis is run for a time period which included the weld run and sufficient time for the plate to cool down to ambient temperature after welding. The resulting thermal analysis loads are further applied during mechanical analysis for evaluation of residual stresses and resulting distortions.

Finite element meshed model used for thermal and mechanical analysis is given in Fig. 13. The symmetry of the welded plate is considered to save the computation time.

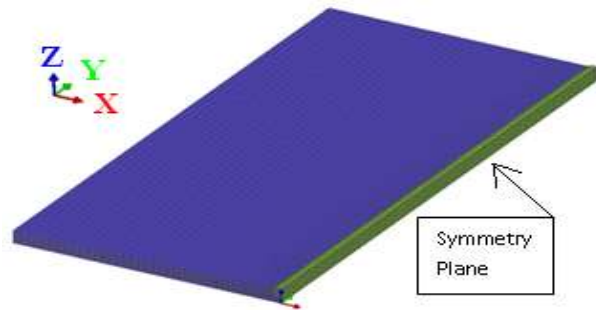


Fig. 13. FEM Meshed Model (Symmetric Half Model)

The isothermal temperature distribution for S355J2G3 welded autogenously is shown in Fig. 14.

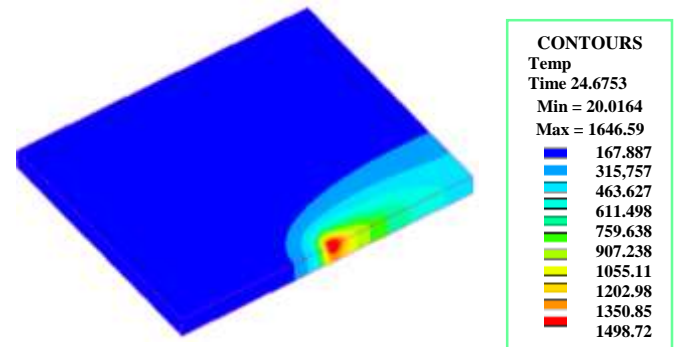


Fig. 14. Isothermal Temperature Distribution Contours for S355J2G3 Autogenously Welded (Symmetric Half Model)

The isothermal temperature distribution for S355J2G3 welded with ER70S6 is shown in Fig. 15.

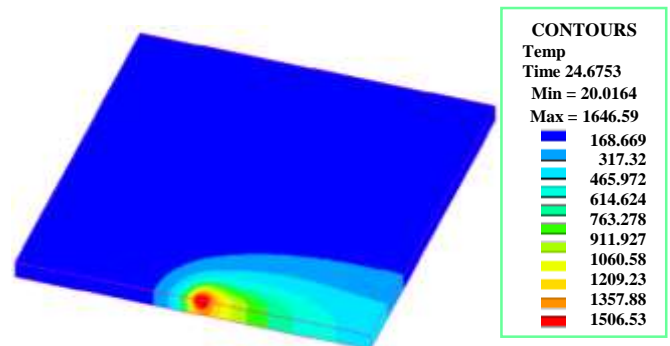


Fig. 15. Isothermal Temperature Distribution Contours for S355J2G3 Welded with ER70S6 (Symmetric Half Model)

C. Mechanical Analysis

After thermal analysis is carried out, thermal loads are being employed on FEA elements for further mechanical analysis for evaluating the stresses developed in the weld specimen like residual stress along with the distortion caused by these loadings. This is a sequential type approach which is commonly employed to simulate the welding process. Other approaches also exist which couple thermal and mechanical loading at the time. This extracted thermal cycle was applied as a thermal loading to each bead according to the welding process.

In the mechanical analysis the clamping conditions (i.e., degrees of freedom constraints) have an important influence on

the evolution of deformations and stresses [23]. Even changing the time of unclamping has an appreciable influence on the residual stresses and deformations. It is obvious that the stiffer the clamping conditions are, the smaller the induced residual deformations are while the stresses are higher. The optimization of the stress-deformation relationship is an important task.

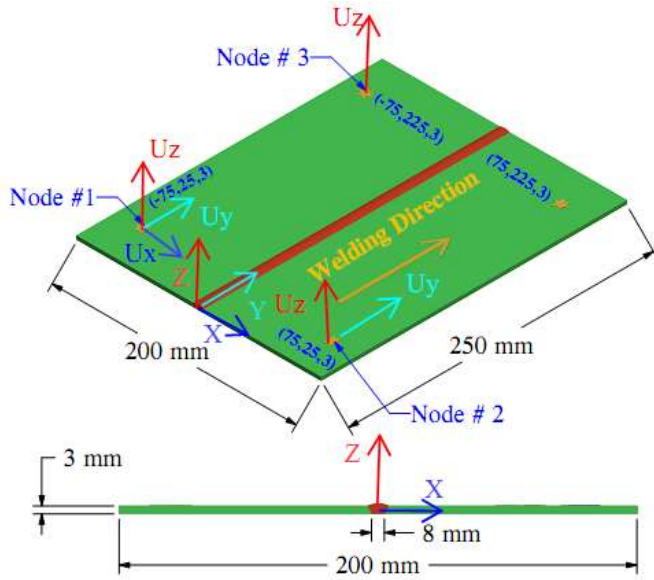


Fig. 16. Clamping as employed in FEM Model for Mechanical Simulation.

For performing any mechanical analysis, the most important consideration is to avoid rigid body motion. Therefore, three nodes have been applied mechanical boundary condition as per location specified in Fig. 16. Among three, node # 1 (50, 25, 0) has been applied with displacement boundary condition, U_{1x} , U_{1y} & U_{1z} . Node #2 (50, 25, 3) has displacement constraints in U_{2x} & U_{2y} , whereas Node #3 has displacement constraints in U_{3z} only. For symmetric problems, as in our case, the nodes are supported in the normal direction of symmetry to save computation time and resources.

D. Welding Distortion Analysis

The simulation was performed for a time period of 3000s. This duration selected so that the weld piece gets enough time to reach the room temperature and resulting welding effects can be analyzed effectively. Automatic time stepping makes the initial time intervals quite small during the deposition of the bead. The successive recordings were taken during the time period. However, when the welding torch finished depositing the bead, the increasingly large time steps are adjusted using the automatic time stepping. This results in non-uniform time steps during the entire welding time.

The vertical distortion response for S355J2G3 welded autogenously-in direction perpendicular to weld center line (WCL)- comes out as 0.25mm as depicted in Fig. 17.

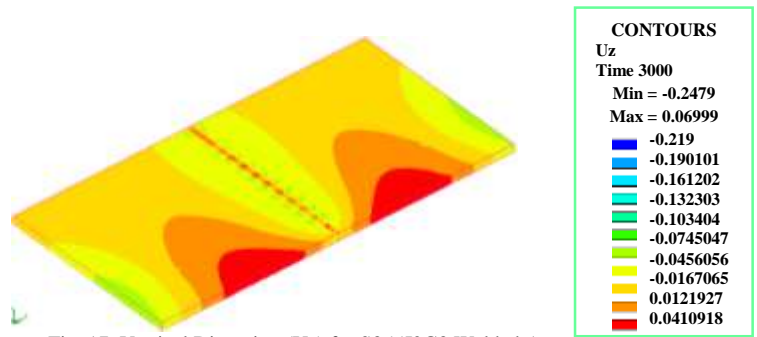


Fig. 17. Vertical Distortion (U_z) for S355J2G3 Welded Autogenously

Vertical distortion response of S355J2G3 welded with ER70S6 is presented in Fig. 18. The distortion in direction perpendicular to weld center line (WCL) comes out as 0.8mm.

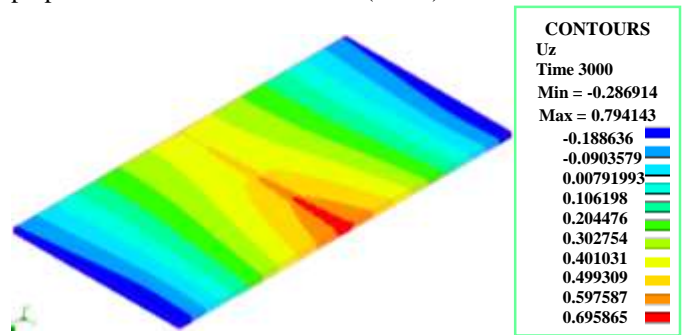


Fig. 18. Vertical Distortion (U_z) for S355J2G3 Welded with ER70S6

E. Welding Residual Stress Analysis

Welding residual stresses generated during autogenous welding of S355J2G3 transverse to weld direction and along the weld direction are presented in Fig. 19 & 20 respectively. Welding residual stresses transverse to weld direction and along the weld direction generated during welding of S355J2G3 with ER70S6 are shown in Fig. 21 & 22 respectively.

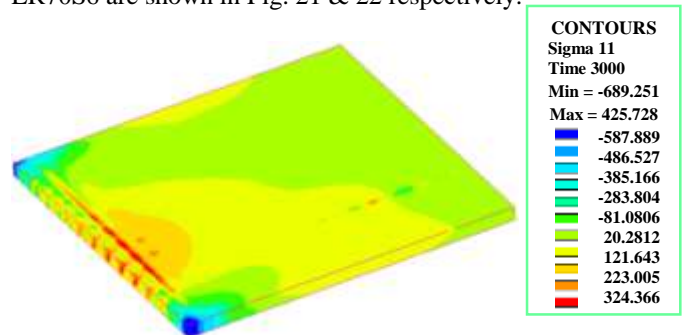


Fig. 19. Welding Residual Stresses (Σ_{11} , Transverse to Weld Dir) in S355J2G3 Welded Autogenously

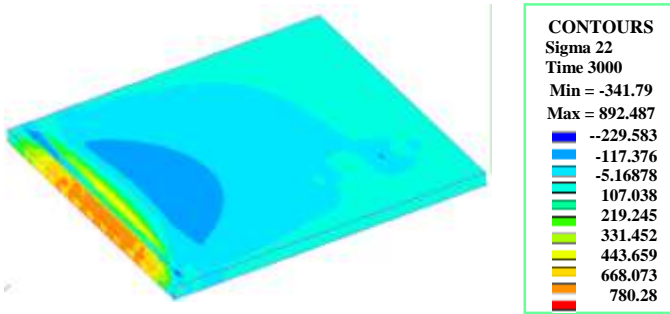


Fig. 20. Welding Residual Stresses (Sigma 22, Along Weld-Dir) in S355J2G3 Welded Autogenously



Fig. 21. Welding Residual Stresses (Sigma 11, Transverse to Weld Dir) in S355J2G3 Welded with ER70S6

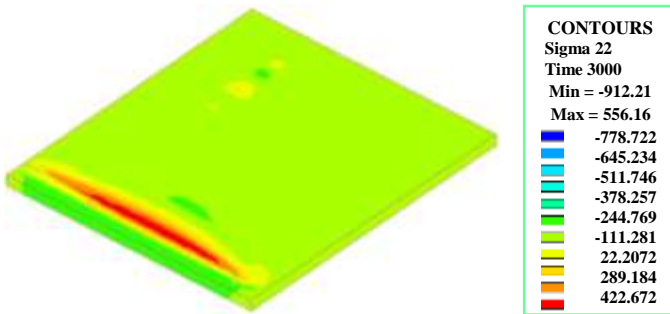


Fig. 22. Welding Residual Stresses (Sigma 22, Along Weld-Dir) in S355J2G3 Welded with ER70S6

Tensile Residual Stresses developed in the weld metals and compressive residual stresses developed in the remaining weld metals. These tensile stresses are developed due to the thermal contraction and hindrance of shrinkage caused by austenite in the molten zone. These stresses can be as high as the yield strength of S355J2G3 In the mechanical analysis the clamping conditions. By decreasing the temperature and beginning of phase transformation, the tensile stress relaxes and approaches to zero and becomes compressive.

IV. RESULTS AND DISCUSSIONS

This section deals with the discussion on the analysis of simulation and experimental results obtained. Firstly, macrograph is discussed and utilization of SYSWELD® Heat Input Fitting Tool to obtain the final heat source parameters to be utilized for further thermal & mechanical analysis of butt welded plate under study. After that a comparison between experimental & simulation temperature distribution has been shown.

A. Weld Macrograph

The region between the blue line for the experimental macrograph represents the heat affected zones, the region between the red line shows the molten zone, whereas, the

remaining area indicate the base metal region. Fig. 23& 24 show comparison between the two cases of the experimental & FEA Weld-Macrograph for both cases.

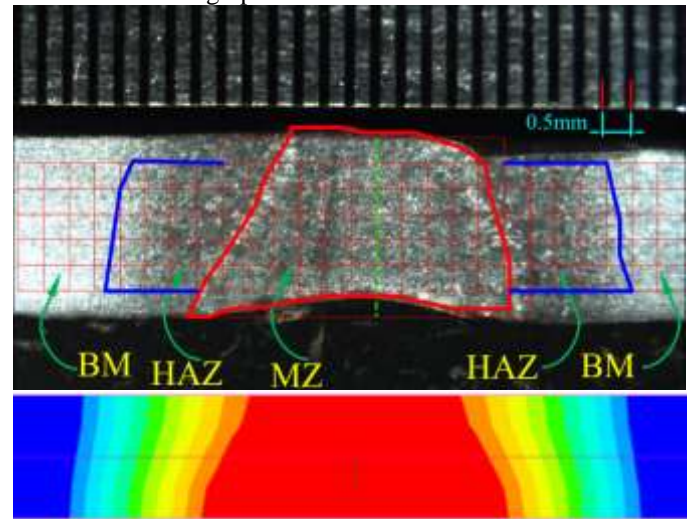


Fig. 23. Experimental & FEA Weld-Macrograph for S355J2G3 Autogenously Welded

The FEA weld macro-graph presented well matches with the obtained from the experiments. This guarantees accurate finite element modeling, as closely to the practical scenarios.

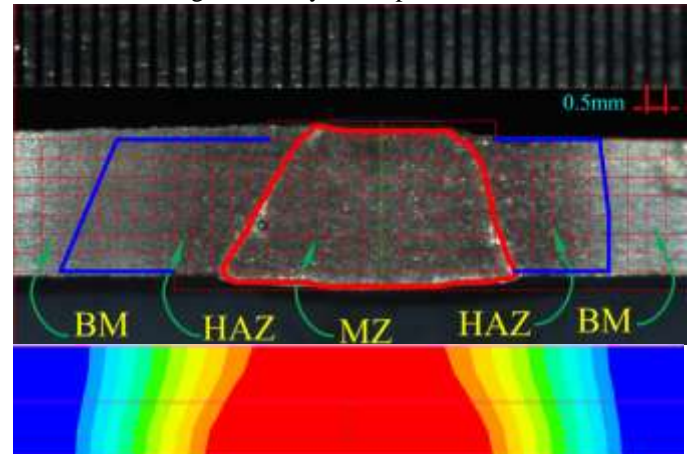


Fig. 24. Experimental& FEA Weld-Macrograph for S355J2G3 Welded with ER 70 S6

B. Temperature Distribution

The temperature distributions for the two welds obtained through experiments is compared with the FEA thermal analyses as shown in Fig. 25 and Fig. 26. The designation employed for temperature measurements in experimental as well as FEA are as follows: N1 stands for Node 1 which lies at 10 mm, N2 stands for Node 2 which lies at 15mm and similarly N3 used for Node 3, which is located at a distance of 20 mm.

There is slight variation in experimental & simulation temperature data. This difference in experimental & simulation temperature increases as the distance increases from the weld centerline. Temperature values obtained from experiments are lower in values as compared to simulated temperature values. This may be due to effect of convection of the air. This reason is also clear when we compare the temperature values at 36 s and at this point both temperature (experimental & simulation)

matches well. The maximum temperature in the molten pools comes out to be 1800 °C. This result has been obtained through simulation. Furthermore, at distance of 20 mm; the difference in peak temperature at this point reaches to about 100 °C, which show excellent agreement.

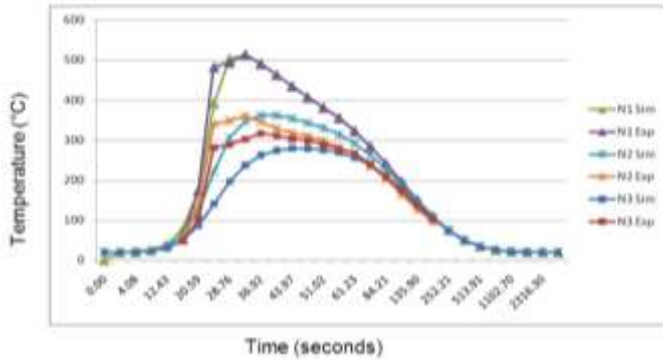


Fig. 25. Experimental & FEA Analysis Temperature Distribution for S355J2G3 Welded Autogenously

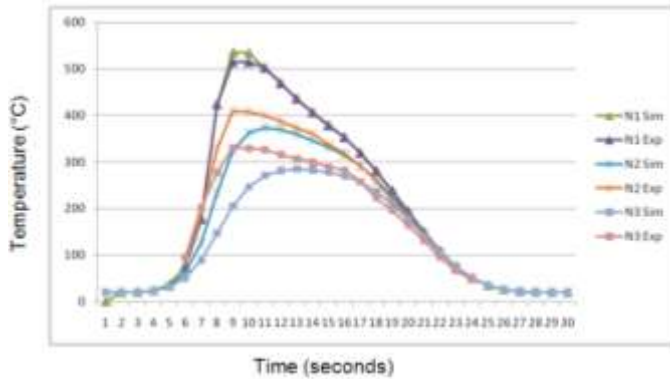


Fig. 26. Experimental & FEA Analysis Temperature Distribution for S355J2G3 Welded with ER 70S6

C. Residual Stresses

In the present work, the X-sectional contour of the Residual Stress Values of Sigma 11 (transverse to weld direction) & Residual Stress Values of Sigma 22 (Stresses along the weld direction) are presented in the Fig. 27 & 28 respectively for S355J2G3 butt-welded plates welded autogenously.

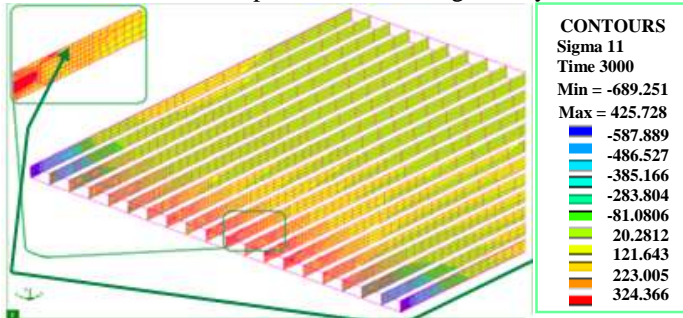


Fig. 27. X-Sectional Contours of Residual Stresses (Sigma 11, Transverse to Weld Dir) in S355J2G3 Welded Autogenously

Tensile Residual Stresses developed in the weld metal and compressive residual stresses developed in the remaining weld metals. This pattern is totally opposite as described earlier for welding of S355J2G3 autogenously. This pattern results because of phase transformation and formation of martensite in the molten zone. The measured residual stresses match quite well with simulated ones when we compare values with Fig. 29.

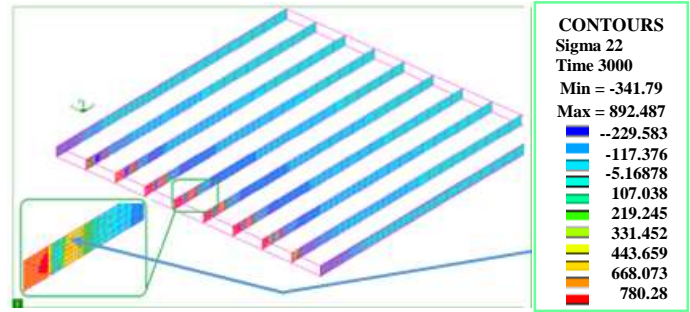


Fig. 28. X-Sectional Contours of Residual Stresses (Sigma 22, Along Weld-Dir) in S355J2G3 Welded Autogenously

Table IV
MEASURED RESIDUAL STRESS VALUES - TP1 - 8MM FROM WELD CENTERLINE

| DEPTH mm | S _{MAX} MPa | S _{MIN} MPa | T _{MAX} MPa | β Deg | S1 MPa | S3 MPa | T13 MPa |
|----------------------|----------------------|----------------------|----------------------|-------|--------|--------|---------|
| Overall up to 1.2 mm | 481 | 89 | 196 | -85 | 91 | 478 | 31 |
| 0.25 | 298 | 45 | 127 | -85 | 47 | 297 | 21 |
| 0.5 | 544 | 84 | 230 | 89 | 84 | 544 | -6 |
| 0.75 | 471 | 84 | 193 | -86 | 86 | 469 | 29 |

Fig. 29. A snapshot of Experimental Residual Stresses by Hole Drill Method for S355J2G3 Welded Autogenously for comparison with FEA results

The X-sectional contour of the Residual Stress Values of Sigma 11 (transverse to weld direction) & Residual Stress Values of Sigma 22 (Stresses along the weld direction) developed for S355J2G3 in the butt-welded plate using Filler ER70S6 are presented in the Fig. 30 & 31 respectively.

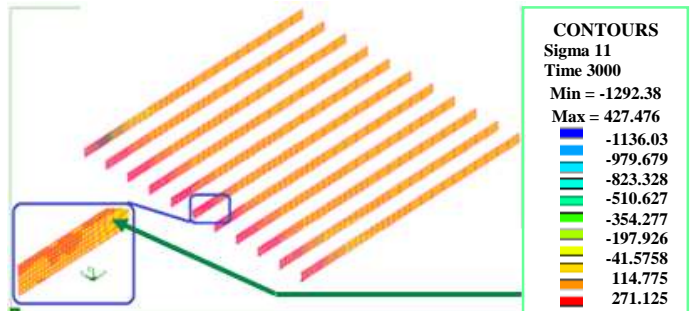


Fig. 30. X-Sectional Contours of Residual Stresses (Sigma 11, Transverse to Weld Dir) in S355J2G3 Welded with ER70S6

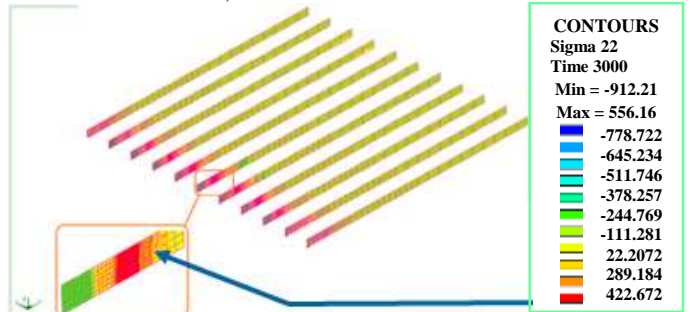


Fig. 31. X-Sectional Contours of Residual Stresses Sigma 22, Along Weld-Dir) in S355J2G3 Welded with ER70S6

Table V
MEASURED RESIDUAL STRESS VALUES - TP2 - 10MM FROM WELD CENTERLINE

| DEPTH | S _{MAX} | S _{MIN} | T _{MAX} | β | S1 | S3 | T13 |
|----------------------|------------------|------------------|------------------|-----|-----|-----|-----|
| mm | MPa | MPa | MPa | Deg | MPa | MPa | MPa |
| Overall up to 1.2 mm | 462 | 168 | 147 | -53 | 273 | 357 | 141 |
| 0.25 | 155 | 61 | 47 | -54 | 93 | 123 | 45 |
| 0.5 | 124 | 20 | 52 | -78 | 24 | 120 | 21 |
| 0.75 | 259 | 105 | 77 | -50 | 168 | 196 | 76 |

Fig. 32. A snapshot of Experimental Residual Stresses by Hole Drill Method for S355J2G3 Welded with ER70S6 Filler for comparison with FEA results

Experimental and finite element analysis (FEA) evaluation of residual stress (tensile in weld metal and compressive in the

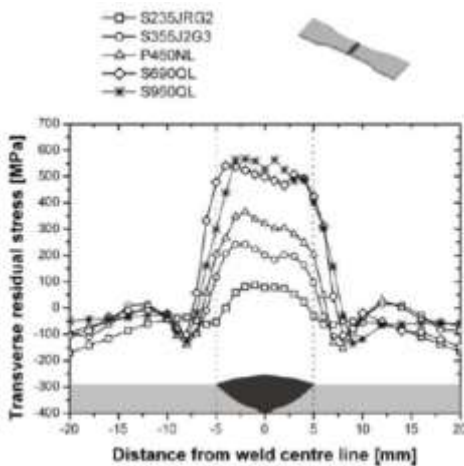


Fig. 33. Residual Stresses in Transverse Direction [24]

remaining weld metals) along transverse and longitudinal direction has been reported by the earlier literature work of Farajian [24] on S355J2G3 and hence validated (These results are being reproduced in the Fig. 33 & 34 respectively).

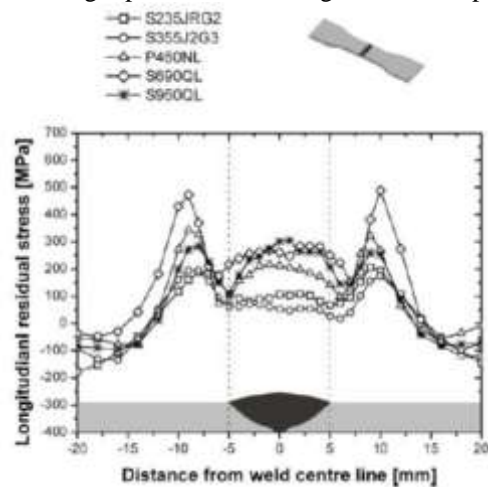


Fig. 34. Residual Stresses in Longitudinal Direction [24]

D. Distortion Analysis

The comparisons of vertical distortion, U_z (Fig. 17) with the experimental measured distortion plot (Fig. 7) shows the quite

good agreement for S355J2G3 welded autogenously. The comparisons of vertical distortion, U_z (Fig. 18) with the experimental measured distortion plot (Fig. 8) gives quite reasonable agreement for S355J2G3 welded with ER70S6.

V. CONCLUSION

In this paper finite element modeling and experimental validation-of temperature distribution, residual stress and distortion in S355J2G3 butt welds using different welding filler configurations-is presented. SYSWELD Heat Input Fitting Tools is employed for obtaining the double ellipsoidal heat source parameters by comparing the experimental weld-macrograph with FEA weld-macrograph.

Residual stresses are measured experimentally using Blind hole drilling method. The results indicate quite high tensile residual stresses developed in the molten zone for welding the plate autogenously as compared to the case for welding with ER70S6 filler and results compared with experimental data. A lesser distortion results when S355J2G3 plate is welded autogenously.

The experimental & finite element analysis results show good agreement for the predicted residual stresses and distortion.

The FEA modelling technique thus developed can be used in future for predicting residual stresses and distortion beforehand for more complex geometries such as pipes-joints, T-joints and joining of large complex structures. Furthermore, it would be equally useful for optimization of welding parameters of heat source for the minimum distortion and/or residual stresses. In future, study can be extended for plate/cylinder of-316 L and other material-by changing the filler (and vice versa) for analysis of temperatures, residual stresses & distortions.

ACKNOWLEDGMENT

The authors are thankful to Chairman SUPARCO, Member Space Electronics & Technology M (SE & T) Wing and Member Space Technology M(ST) Wing for the guidance and technical supports. Special thanks are also due to DDG (SM), Director (FEMF), DH(EVT), DDG Manufacturing, Director (Fabrication and Welding), DG (QA & MR) for providing immense moral support and encouragement throughout this research work.

In addition, special thanks to the QA & MR Team, Prop Dte Gen Team and many others who have assisted for measurement of residual stresses & Data Acquisition of Temperatures and other works during this experimental work.

REFERENCES

- [1] H. B. Cary, *Modern Welding Technology*, Third. Prentice Hall Inc, 1994.
- [2] American Welding Society, "Volume-1 Welding Science and Technology," in *Welding Hand Book*, Ninth Edit., C. L. Jenney and A. O'Brien, Eds. American Welding Society, 2001, pp. 298-300, 314.
- [3] E.F. Rybicki, J.R. Shadley, "A three-dimensional finite element evaluation of a destructive experimental method for determining through-thickness residual stresses in girth welded pipes" *Journal of Engineering Materials and Technology, ASME, America*, vol. 108/99, April 1986.
- [4] Y. Shim, Z. Feng, S. Lee, D. Kim, J. Jaeger, J. C. Papritan, C. L. Tsai, "Determination of residual stresses in thick-section weldments" *Welding*

- Journal*, American Welding Society and the Welding Research Council, September 1992, pp. 305.s -312. s.
- [5] Li Yajiang, Wang Juan, Chen Maoai, Shen Xiaoqin, "Finite element analysis of residual stress in the welded zone of a high strength steel," *Indian Academy of Sciences, Bull. Mater. Sci.*, vol. 27, no. 2, pp. 127–132, April 2004
 - [6] D. Stamenković, I. Vasović, "Finite element analysis of residual stress in butt welding two similar plates," *Scientific Technical Review*, vol. LIX, no.1,2009.
 - [7] M.N. Chougule, S.C. Somase, "Experimental and analytical study of thermally induced residual stresses for stainless steel grade using GMAW process," in *5th International & 26th All India Manufacturing Technology, Design and Research Conference*, IIT Guwahati, Assam, India, December 12th -14th, 2014, pp. 674.1-674.6.
 - [8] N. Jayakumar, S. Mohanamurugan, R. Rajavel, J. Ashok Kumar, "Residual stress analysis in austenitic stainless steel weldment by finite element method," *Indian Journal of Science and Technology*, vol. 8(36), December 2015.
 - [9] S.-H. Cho and J.-W. Kim, "FEM prediction of welding residual stress and distortion in carbon steel considering phase transformation effects," *Materials & Design - Journal - Elsevier* 30 (2009) pp. 359–366.
 - [10] G. Apostol, G. Solomon, D. Iordăchescu, *Input parameters influence on the residual stress and distortions at laser welding using finite element analysis*, U.P.B. Sci. Bull., Series D, vol. 74, Iss. 2, 2012.
 - [11] Varma Prasad V.M., Joy Varghese V.M., Suresh M.R. Siva Kumar D., "3D simulation of residual stress developed during TIG welding of stainless steel pipes," in *International Conference on Emerging Trends in Engineering, Science and Technology (ICETEST - 2015)*, Procedia Technology 24 (2016), pp. 364 – 371.
 - [12] Rafiqul Islam Mohammed, "Finite Element Analysis of Fillet Welded Joint," Bachelor of Engineering (Mechanical) dissertation, Faculty of Health Eng., and Sci., University of Southern Queensland, Toowoomba, Queensland, Australia, 2015.
 - [13] Davood Azadi, Nosratollah Solhjoei, Sayed Ali Mousavi, "Experimental study and finite element simulation of residual stress in welded sections of steel p91 pipes with multi-pass welding," *Int. Journal of Advanced Design and Manufacturing Technology*, vol. 9/ No. 3/ September–2016.
 - [14] A. M. A. Pazooki, M. J. M. Hermans, I. M. Richardson, "Finite element simulation and experimental investigation of thermal tensioning during welding of DP600 steel," in *Science and Technology of Welding and Joining*, Taylor & Francis (ISSN: 1362-1718), May 2016.
 - [15] Wenchun Jiang, Yun Luo, J. H. Li, Wanchuck Woo, "Residual stress distribution in a dissimilar weld joint by experimental and simulation study," *Journal of Pressure Vessel Technology*, vol. 139 / 011402-1, February 2017.
 - [16] Kyoung-soo Lee1, W. Kim, Jeong-geun Lee, Chi-yong Park, Jun-seok Yang, Tae-ryong Kim, Jai-hak Park, "Finite element analysis and measurement for residual stress of dissimilar metal weld in pressurizer safety nozzle mockup," *Journal of Mechanical Science and Technology* 23 (2009) pp. 2948~2955.
 - [17] J. Mathar. "Determination of Initial Stresses by Measuring the Deformation Around DrilledHoles." *Transactions of the American Society of Mechanical Engineers*, Vol.56, No.4,pp.249-254, 1934.
 - [18] W. Zang, J. Gunnars, P. Dong, and J. K. Hong, "Improvement and Validation of Weld Residual Stress Modelling Procedure," 2009.
 - [19] G. Vishay Precision, "Measurement of Residual Stresses by the Hole-Drilling * Strain Gage Method TN-503-6," *Tech Note TN-503*, 2010.
 - [20] Determining Residual Stresses by the Hole-Drilling Strain-Gage Method, ASTM Standard Test Method E837-99. *American Society for Testing and Materials*. 1999.
 - [21] Nitschke-Pagel and H. Wohlfahrt, "The generation of residual stresses due to joining process, Residual stress measurement, calculation and evaluation," *DGM-informationsgesellschaft Verlag*, vol. 1, pp. 121-134, 1991.
 - [22] N. Nguyen et al, "Analytical solution of double-ellipsoidal moving heat source and its use for evaluation of residual stresses in bead-on- plate.," in *International conference on fracture mechanics and advanced engineering materials*, University of Sydney, Australia, 1999.
 - [23] Denes Kollar, "Numerical Simulation of Welding Process Application in Buckling Analysis," *Periodica Polytechnica Civil Engineering*, 61(1), pp. 98-109, 2017.
 - [24] M. Farajian, "Welding residual stress behavior under mechanical loading," in *Commission XIII Fatigue of welded components and structures*, International Institutes of Welding , Paris, 2012.